Bubble Nucleation and Growth Anomaly for a Hydrophilic Microheater Attributed to Metastable Nanobubbles

Richard E. Cavicchi

National Institute of Standards and Technology, 100 Bureau Drive, Gaithersburg, Maryland 20899, USA

C. Thomas Avedisian*

Sibley School of Mechanical and Aerospace Engineering, Cornell University, Ithaca, New York 14853-7501, USA

(Received 21 April 2006; revised manuscript received 27 December 2006; published 19 March 2007)

Nanobubbles on a hydrophilic surface immersed in water and ethanol are inferred from the response of the surface to two consecutive heat pulses with a variable separation time. Bubble nucleation occurs at specific positions on the surface during the first heat pulse but at lower nucleation temperatures and random locations on the second. Nanobubbles are hypothesized to form on collapse of the bubble from the first pulse.

DOI: 10.1103/PhysRevLett.98.124501 PACS numbers: 47.55.db, 64.60.My, 64.60.Qb, 68.08.Bc

The concept of nanodimensioned bubbles—nanobubbles—was first used to explain the long range discontinuities or steps in the attractive forces between hydrophobic surfaces observed during controlled separation of two surfaces initially in contact [1]. Nanobubbles have subsequently been conjectured to exert an important influence on a number of technological applications, for example, as a means to promote slip at surfaces and reduce significantly the shear stress and drag [2–4].

Because of the small size of nanobubbles, the information revealing their existence is circumstantial and indirect. Atomic force microscopy (AFM) operating in the ''tapping'' mode revealed structures on silanated glass suggestive of nanobubbles between the two surfaces [5,6]. Later interpretation of these results by Evans *et al.* [7] noted that AFM measurements of adhesion forces could be explained by formation of a polydimethylsilane film created by condensation of atmospheric moisture on the surface. As further evidence of the evolving nature of the current understanding of nanobubbles and the metrology used to study them, Holmberg *et al.* [8] reported for the first time that AFM operating in the so-called ''contact mode'' can be made to show the presence of nanobubbles by adjusting the scanning force.

The work described here is motivated by the observation that nanobubbles have thus far only been observed on hydrophobic surfaces (i.e., surfaces for which the contact angle in the liquid is greater than about 90°) as contrasted with hydrophilic surfaces (contact angle less than 90°) where no nanobubblelike structures are evident from AFM scans (e.g., [7]). Hydrophilic surfaces are apparently not conducive to promoting bubble stability because bubble detachment and dissolution is favored as a surface becomes more hydrophilic [9,10]. We expect that if nanobubbles can exist on hydrophilic surfaces they would be comparatively unstable and their appearance momentary. A process is required for understanding the presence of nanobubbles at a hydrophilic surface that is sufficiently rapid to reveal the influence of the bubbles during their short lifetime. We suggest here that bubble nucleation under pulse heating conditions provides such a process.

The procedure of the experiment is to impulsively heat a thin metal film immersed in a fluid for a controlled duration τ (5 μs in this case), using two consecutive heat pulses separated by a time τ_p. Differences in the evolution of surface temperature between the first and second pulses are used to infer the presence of nanobubbles at the surface. With impulsive heating, the influence of gas pockets in surface imperfections that can act as nucleation sites is minimized [11]. By adjusting τ_p we observe a statistical variation of the nucleation temperature for the second pulse and a more chaotic arrangement of microbubbles at the surface that is conjectured to be due to metastable nanobubbles formed by collapse of bubbles after the first pulse. Analysis of bubble collapse predicts formation of shock waves [12,13] and/or a damped collapse to a nonzero equilibrium size [14] under certain conditions, either process of which can be a mechanism to form much finer bubbles. We note that a double-pulse bubble nucleation process was also employed by Yavas *et al.* [15] to document a ''memory'' (or reversible heating) effect for water in contact with a Cr film. It was conjectured that ''metastable ultramicroscopic bubbles'' formed during the first pulse were responsible for differences between the two pulses.

The hardware used was described previously [16,17]. The primary modification is the capability to impose a second pulse after a time τ_p. The heater consists of a platinum (Pt) film 2000 Å thick, 15 μm wide, and 30 μm long on an insulating layer of SiO_2. The Pt film forms one side of a bridge circuit to which an input voltage $V_{\text{in}}(t)$ is introduced for a specified τ to electrically heat the film. V_{in} is selected to promote bubble nucleation at about 0.95τ as a reference point. V_{out} from the bridge is moni-

tored and an inflection point in $V_{out}(t)$ indicates bubble nucleation [18]. The fluids are water, ethanol, and hexane which have a range of contact angles and surface wettabilities. Bare Pt is hydrophilic in water (e.g., contact angle of about 40 °C at room temperature [19]). For the high superheats typical of rapid evaporation at the superheat limit (order of 200 °C or more for water [20]) ethanol, hexane, and water should continue to maintain their hydrophilicity on Pt or become more strongly hydrophilic. We also examined Pt coated by a self-assembled hydrophobic monolayer [hexadecanethiol (HDT)] in a process described by Balss *et al.* [17]), and Pt roughened by an ion beam.

V_{out} can be related to the film temperature through a separate calibration of resistance with temperature using standard equations of bridge circuitry [16]. Assuming a linear relation between the resistance of the Pt film and temperature of the film T_f, and selecting the resistors in the bridge circuit so that the balance resistors are much larger than the potentiometer and Pt film resistors, it can be shown that $\Delta T(t) \approx \frac{V_{out}(t)}{V_{in}(t)} C$ where $\Delta T = T_f - T_0$, T_0 is a reference temperature (e.g., room temperature) and C is a constant. We thereby frame the discussion of Pt film temperature in response to V_{in} entirely in terms of V_{out}. For $\tau_p > 10$ μs and V_{in} sufficiently low (i.e., <3.85 V), we found that the Pt heater returned to ambient temperature before the start of the second pulse since $V_{out1} = V_{out2}$. At shorter separation times the surface temperature had not cooled sufficiently, similar to high frequency periodic heating and short separation time conditions [21].

We infer the presence of nanobubbles by comparing $V_{out1}(t)$ and $V_{out2}(t)$ with differences thought to be due to variations of surface conditions that are triggered by bubble nucleation. Visualizations of bubble morphology during the heating pulses were also obtained to determine the extent of surface coverage of nucleated bubbles using a laser flash technique [17,22]. The surface coverage of the observable microbubbles may be indicative of nanobubbles from whence the microscopic bubbles could have originated.

Figure 1(a) shows the evolution of V_{out1} and V_{out2} for two consecutive pulses with $\tau_p = 30$ μs and $V_{in} = 4.15$ V (for both pulses). For these conditions, there is no inflection in V_{out1}, $V_{out1}(t) \approx V_{out2}(t)$ and single phase heating conditions prevail for both pulses. At $V_{in} = 4.25$ V observable differences of V_{out1} and V_{out2} arise as shown in Fig. 1(b). An inflection point indicating bubble nucleation during both pulses is now present (signified by the horizontal line), and nucleation occurs much earlier for the second pulse compared to the first pulse. As a consequence $V_{peak2} > V_{peak1}$ because the insulating effect of the bubble for the second pulse acts over a longer period on the surface compared to the first pulse.

The lower inflection point voltage for the second pulse in Fig. 1(b) suggests a difference in surface condition for the two pulses which we believe is brought about by the

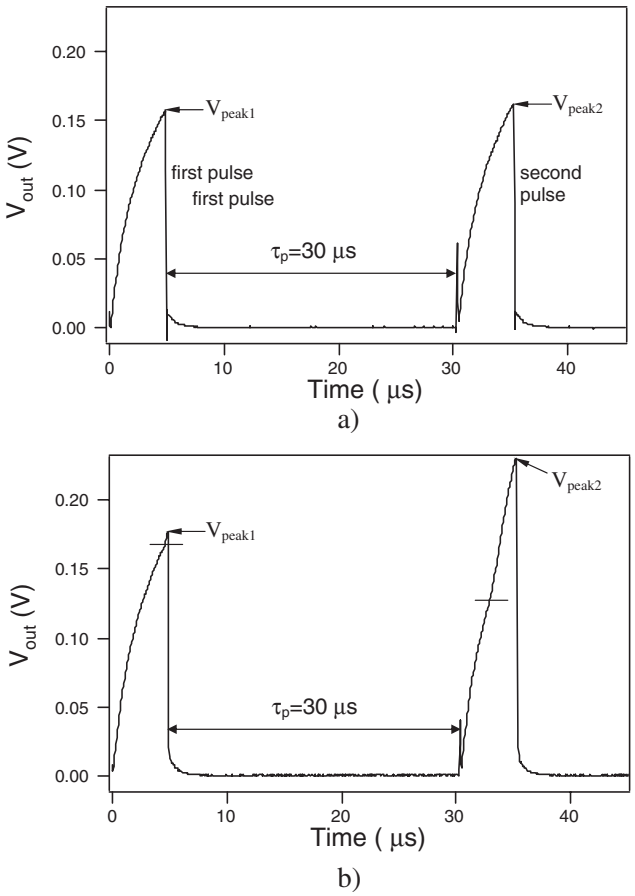

FIG. 1. (a) Evolution of V_{out} for a 2-pulse sequence for $V_{in} = 4.15$ V; (b) evolution of V_{out} for a 2-pulse sequence for $V_{in} = 4.25$ V. The horizontal line indicates the inflection point.

bubble collapse process associated with termination of the first pulse. We know that at 30 μs the surface has cooled to ambient after the first pulse. High speed photomicroscopy shows that the time for observable collapse of a bubble formed under similar pulse heating conditions is on the order of a time slightly longer than τ [17,22]. The conjecture is that metastable nanobubbles formed as a result of collapse from the first pulse are distributed on the surface at the start of the second pulse. The bubbles are metastable because if we make τ_p long enough, then $V_{out1}(t) = V_{out2}(t)$ which signifies that the initial conditions for both pulses are identical. However this process may evolve, it would be a combination of bubble nucleation, growth, and collapse at length scales similar to the intermolecular region the understanding of which may benefit from molecular dynamics simulations [23].

While $V_{out1}(t)$ is stable and reproducible, we observe a statistical variation from pulse to pulse in $V_{out2}(t)$. Figure 2 shows inflection point temperatures of ten consecutive double pulses for $\tau_p = 201.3$ μs as a reference on a bare Pt surface in water. The inflection point temperature of the second pulse is significantly lower than for the first pulse. This variation suggests a statistical distribution of nano-

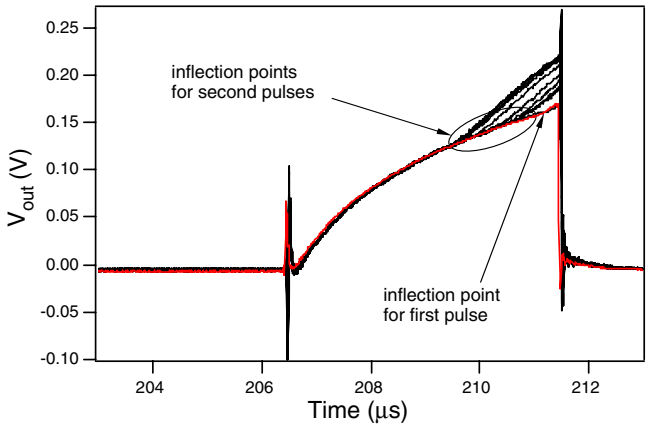

FIG. 2 (color online). Evolution of V_{out2} for 10 different signals obtained at $\tau_p = 200$ μs. The line (red online) is the response to the first pulse.

bubble sizes, with different nucleation temperatures being associated with different bubble sizes. As shown in Fig. 2, prior to bubble nucleation (i.e., single phase liquid for $t <$ 209 μs) the response for all ten pulses is identical and the same as $V_{out1}(t)$ indicating that nanobubbles are present. If a nanovapor barrier is present at the surface as described in [24], it could perhaps produce a small change in both $V_{out1}(t)$ and $V_{out2}(t)$ while not affecting the difference between $V_{out1}(t)$ and $V_{out2}(t)$.

Figure 3(a) shows the bubble morphology associated with the first pulse of a two pulse sequence (duration of each pulse is 5 μs). Each photograph in Fig. 3(a) is taken 4.4 μs after initiation of the first pulse. The behavior of the first pulse is the same as if $\tau_p \rightarrow \infty$. A rather orderly nucleation process at a specific location at the surface is shown for the first pulse [Fig. 3(a)] and the bubble size and location do not change from pulse to pulse. Photographs taken at later times (not presented here) showed bubbles that grew until they covered the entire surface, followed by collapse and disappearance after the heat pulse was turned off. Figure 3(b) shows images of bubbles formed during a second pulse triggered at $\tau_p = 45$ μs. The bubbles in Fig. 3(b) show significant randomness as to the location, size, and number of microbubbles. We believe this randomness is responsible for the statistical variation of nucleation temperature illustrated in Fig. 2. It is interesting that a "rim" surrounds the microbubbles which form during the second pulse as shown in Fig. 3(b), unlike for the bubbles formed during the first pulse [Fig. 3(a)]. We are not sure why this rim forms, but since it is only observed for the second pulse, the rims are evidently triggered by the differing surface conditions between the first and second pulses.

It was indicated that nanobubbles could serve as nucleation sites. Precisely how this could occur is open to speculation. A nanobubble could serve as an embryo for a phase change process with the corresponding metastable state

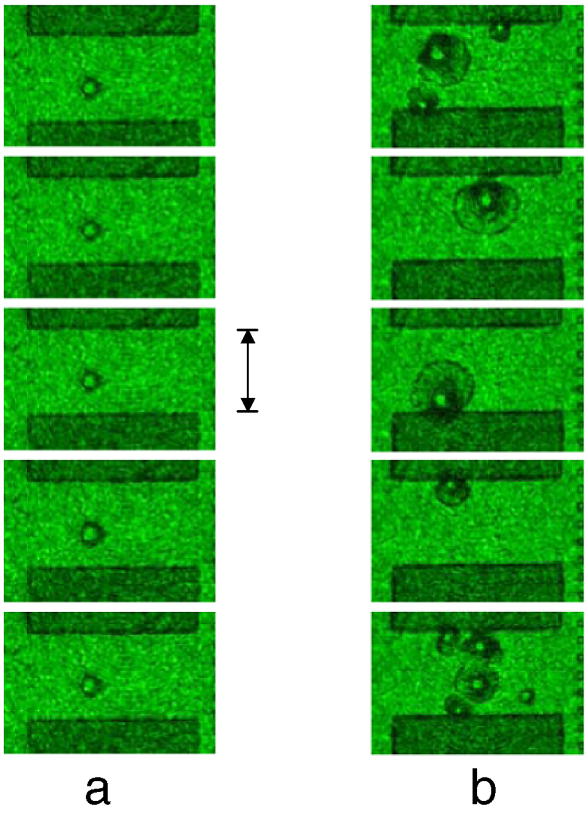

FIG. 3 (color online). (a) Photographs showing bubble morphology from the first pulse of a two-pulse sequence each taken at the same time (4.4 μs) after initiation of a 5 μs pulse to illustrate repeatability. The exposure time for each photograph was 7.5 ns. The vertical bar indicates 15 μm. (b) Photographs from the second pulse of a two-pulse sequence each taken at the same time (2.9 μs) after initiation of a 5 μs pulse for $\tau_p =$ 45 μs (i.e., each photograph was taken 47.9 μs after the end of the first pulse) to illustrate bubble morphology and location on the surface. The exposure time for each photograph was 7.5 ns.

determined by a balance of forces acting on the surface of the bubble. The Laplace Young equation [25] defines such a state: $P(T) \approx P_0 + \frac{2\sigma(T)}{R}$ where R would be the bubble radius, or a characteristic dimension of surface roughness, $P(T)$ is the temperature-dependent pressure inside of the bubble, P_0 is the ambient pressure (1 atm in our study), and $\sigma(T)$ is surface tension. We measured the surface roughness of our bare Pt films by AFM and found it to be about 1.3 nm. Surfaces that had been roughened by ion-beam treatment were also examined with corresponding roughnesses increasing to about 2.6 nm. For either value, and using the properties of water for illustration [26,27], we calculate a nucleation temperature that is much higher than measured indicating that roughness on this scale does not act as nucleation sites. Larger bubbles (~10 nm) lead to predicted temperatures of about 254 °C, which is more consistent with surface temperatures produced by single pulse measurements in water [18] (i.e., $\tau_p = \infty$).

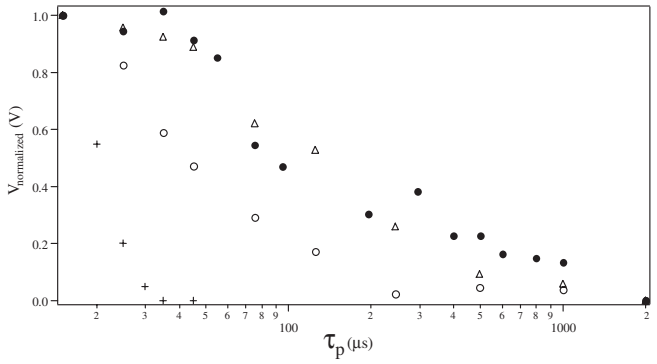

FIG. 4. Variation of V_{peak} with τ_p for the following surfaces: +, ethanol on untreated Pt; ○, water on untreated Pt; △, water on hydrophobic HDT monolayer; ●, water on ion-beam roughened Pt.

The difference in the peak amplitudes, V_{peak2}-V_{peak1} expressed as $V_{normalized}$ $(=[V_{peak2}(\tau_p)\text{-}V_{peak1}]/[V_{peak2}(15\ \mu s)\text{-}V_{peak1}])$, decreases with τ_p as shown in Fig. 4 [$V_{peak2}(15\ \mu s)$ is an arbitrary reference]. The longest lifetime of the nanobubbles is observed for thiol and a Pt surface roughened by an ion beam, the similarity of which suggests that roughening makes the surface more hydrophobic. Ethanol shows a comparatively shorter lifetime. All the fluids have $V_{normalized} = 0$ for $\tau_p > 1$ ms. For hexane (data not shown in Fig. 4), we found that $V_{normalized} = 0$ for the range of τ_p examined which indicates that any effect from nanobubbles is completely suppressed. Analysis of bubble dynamics (in the bulk of a liquid) leads to a stability condition for bubble collapse to a finite size [14]. Hexane is farther from the stability condition than water or ethanol so hexane bubbles should more readily completely collapse. Furthermore, hexane wets better than water on Pt, which should result in more pronounced penetration of hexane into surface features, possibly also displacing nanobubbles and, if so, reducing the influence of nanobubbles on the bubble nucleation process. That $V_{normalized} = 0$ for hexane is consistent with these trends.

In conclusion, we have observed changes in the nucleation process of bubbles on a hydrophilic, pulse-heated surface following the collapse of a bubble from a previous pulse. These changes, which include depressed nucleation and higher peak temperatures, and statistical variations of bubble morphology for identical drive pulses, are suggested to be indicative of metastable nanobubbles that are present for about 1 ms.

The authors acknowledge Dr. Michael J. Tarlov for helpful discussions, Dr. Jaroslaw Grobelny for AFM scans of the Pt films, and Mr. Christopher Montgomery for ion-beam treatment and device preparation. One of the authors (C. T. A.) acknowledges partial support from the New York State Institute of Biotechnology and Life Science Technologies.

*Corresponding author.
Email address: cta2@cornell.edu

[1] J. L. Parker, P. M. Claesson, and P. Attard, J. Chem. Phys. **98**, 8468 (1994).
[2] E. Lauga and H. A. Stone, J. Fluid Mech. **489**, 55 (2003).
[3] E. Lauga and M. P. Brenner, Phys. Rev. E **70**, 026311 (2004).
[4] P. G. de Gennes, Langmuir **18**, 3413 (2002).
[5] P. Attard, M. P. Moody, and J. W. G. Tyrell, Physica (Amsterdam) **314A**, 696 (2002).
[6] J. W. G. Tyrrell and P. Attard, Phys. Rev. Lett. **87**, 176104 (2001).
[7] D. R. Evans, V. S. J. Craig, and T. J. Senden, Physica (Amsterdam) **339A**, 101 (2004).
[8] M. Holmberg, A. Kuhle, J. Garnaes, K. A. Morch, and A. Boisen, Langmuir **19**, 10510 (2003).
[9] T. Baum and D. J. J. Schiffrin, J. Micromech. Microeng. **7**, 338 (1997).
[10] B. Budhlall, X. He, I. Hyder, S. Mehta, and G. Parris, in *Proceedings of the International Symposium on Immersion and 157 nm Lithography, Vancouver, British Columbia, Canada, 2004*, File No. 2-05, http://www.sematech.org/meetings/archives/litho/immersion/20040803/index.htm
[11] A. Asai, J. Heat Transfer **113**, 973 (1991).
[12] C. C. Wu and P. H. Roberts, Phys. Rev. Lett. **70**, 3424 (1993).
[13] B. P. Barber and S. J. Putterman, Phys. Rev. Lett. **69**, 3839 (1992).
[14] V. A. Bogoyavlenskiy, Phys. Rev. E **60**, 504 (1999).
[15] O. Yavas, P. Leiderer, H. K. Park, C. P. Grigoropoulos, C. C. Poon, and A. C. Tam, Phys. Rev. Lett. **72**, 2021 (1994).
[16] O. C. Thomas, R. E. Cavicchi, and M. J. Tarlov, Langmuir **19**, 6168 (2003).
[17] K. M. Balss, C. T. Avedisian, R. E. Cavicchi, and M. J. Tarlov, Langmuir **21**, 10459 (2005).
[18] C. T. Avedisian, W. S. Osborne, F. D. McLeod, and C. M. Curley, Proc. R. Soc. A **455**, 3875 (1999).
[19] A. W. Adamson and A. P. Gast, *Physical Chemistry of Surfaces* (John Wiley & Sons, New York, 1997), 6th ed., pp. 365 and 369.
[20] C. T. Avedisian, J. Phys. Chem. Ref. Data **14**, 695 (1985).
[21] T. J. Fisher, C. T. Avedisian, and J. P. Krusius, IEEE Trans. Components, Packaging B **19**, 255 (1996).
[22] C. T. Avedisian, R. E. Cavicchi, and M. J. Tarlov, Rev. Sci. Instrum. **77**, 063706 (2006).
[23] V. Carey and A. P. Wemhoff, Int. J. Heat Mass Transf. **48**, 5431 (2005).
[24] Z. Ge, D. G. Cahill, and P. V. Braun, Phys. Rev. Lett. **96**, 186101 (2006).
[25] P. G. Debenedetti, *Metastable Liquids* (Princeton University Press, Princeton, NJ, 1996), pp. 176–187.
[26] J. H. Keenan, F. G. Keyes, P. G. Hill, and J. G. Moore, *Steam Tables* (John Wiley & Sons, NY, 1969).
[27] N. B. Vargaftik, B. N. Volkov, and L. D. Voljak, J. Phys. Chem. Ref. Data **12**, 817 (1983).